2010 SCEC FINAL REPORT

Project Title: "L. A. Basin Short-Period Seismology"

Don Helmberger, Principal Investigator

In this report, we will cover past efforts which have now been published or about to, and their relationship to the current LA Basin project.

(a) Review of long-period efforts (>5s)

Here, we briefly review the methodology of "CAPloc", for both retrieval of source parameter and location. Let $u(t)$ be a recorded seismogram with instrument response removed. The corresponding synthetics, $s(t)$, for a double couple source can be expressed as a summation of contributions from three fundamental faults, namely, vertical strike-slip, vertical dip-slip, and 45° dip-slip:

$$s_j(t) = M_0 \sum_{i=1}^{3} A_{ij}(\phi - \varphi(\theta,\xi),\delta,\lambda) G_{ij}(h,\Delta(\theta,\xi),t) \qquad (1)$$

where j = 1, 2, 3 denotes the vertical, radial, and tangential component, respectively [*Helmberger*, 1983]. The G_{ij}'s are the Green's functions, and the A_{ij}'s are the radiation coefficients. M_0 is the scalar moment. φ and Δ are the station azimuth and distance. The unknowns, h (depth), ϕ(strike), δ(dip) and λ(rake), that describe the source depth and orientation, together with θ(event latitude) and ξ(event longitude) that define the epicenter location, can be obtained by solving the equation

$$u(t) = s(t). \qquad (2)$$

We solve Eqn. 2 in a grid-search manner where a weighted summation of waveform misfit errors (e_{Pnl} and e_{Sur} defined in Eqn.3) plus P-wave travel time residues are minimized.

$$e_{Pnl} = \left\| u^{Pnl}(t) - s^{Pnl}(t - \Delta T) \right\|$$
$$e_{Sur} = \left\| u^{Rayleigh}(t) - s^{Rayleigh}(t - \Delta T - \delta t^{rayleigh}) \right\| + \left\| u^{Love}(t) - s^{Love}(t - \Delta T - \delta t^{Love} \right\| \qquad (3)$$

Here $\| \ \|$ denotes the L_2 norm. ΔT is the time shift to align synthetics with data on the first P arrival. The $\delta t^{Rayleigh}$ and δt^{Love} stand for the path specific timing corrections for the synthetic Rayleigh and Love wave segments from calibration. We distinguish body (Pnl) and surface waves because they sample the crustal structure differently and provide independent constrain on the source parameters. To take full advantage of both Pnl and surface waves, an adaptive weighting scheme between them was developed and proved crucial when a sparse data set is used (see *Tan et al.*, 2006). The first stage in the use of Eqn. 3 is to establish the phase-delays (δt's), a calibration and mapping procedure so that these delays can be estimated for any path ending at (θ, ξ).

The calibration can be obtained from past earthquakes (over 200 events) with reasonably known locations as given in *Tan et al.* (2010) or from Ambient Seismic Noise, *Zhan et al.* (2011). The latter paper has been accepted for publication in BSSA (June issue). A comparison of P-wave pick locations against the Earthquake Centroid locations for a large population of events has been submitted, *Wei et al.* (2011). We also address the issues involving station sampling in both location and mechanism.

(b) Short-period inversions

The characterization of small events (Mw>3.5) remains a particular challenge because their fault lengths are generally less than a few hundred meters. Yet these small events are the primary provider of fundamental information about fault zones. To study such detailed features requires modeling at high frequency where surface conditions beneath the recording sites contaminate the source information. We have developed a hybrid approach using empirical path corrections. The process is iterative where Long-Period solutions (LP, 5s and longer) are used to calibrate (.5 to 2 Hz) followed by extension to (2-8 Hz). To achieve this, we have expanded the Cut-And-Paste (CAP) methodology to include not only timing shifts but amplitude corrections in various frequency bands, called CAP+ and CAP++. *Tan & Helmberger* (2007) demonstrate that accurate mechanisms can be determined down to small events (M < 2) with these calibrations.

Tan and Helmberger (2010) developed a forward modeling technique which fully utilizes both duration and amplitude information to estimate rupture directivity. The *a priori* Haskell source model proves appropriate for most events that they have studied of the 2003 Big Bear sequence and facilitates estimation of rupture parameters, such as fault length (fl) and rupture speed (Vr).

In particular, we conduct a grid search to solve for a common rise time τ_r and rupture duration time τ_c at individual stations that minimize the total waveform misfit error

$$e = \sum_{i=1}^{N} (d_i(t) - \Delta M_0 g_i(t) \otimes (\tau_r \otimes \tau_c)) . \quad (4)$$

Here $d_i(t)$ and $g_i(t)$ represent records from the mainshock and the EGF event. ΔM_0 is a scaling factor to account for the difference in size and radiation pattern of the two events. The summation is over the available stations. Note that $\tau_r \otimes \tau_c$ gives the relative source time function (RSTF) of the mainshock with respect to the aftershock. In the simple scenario of unilateral horizontal rupture on a vertical fault, the variation of τ_c s can be modeled with

$$\tau_c = \frac{fl}{V_r} - \frac{fl}{V_{p,s}} \cos(\varphi - \phi) , \quad (5)$$

where fault length (fl) and rupture speed (V_r can be easily estimated. φ and ϕ from eqn. (5) are the rupture propagation direction and the station azimuth respectively.

The results for the Big Bear Sequence is published in *Tan & Helmberger* (2010) where they find a relationship between *fl* and rupture velocity. Essentially, events on the main older fault zones have low stress drops with fast rupture velocities while new faults have high stress drops and low rupture velocities.

This same procedure was applied to the 2008 (M_w = 4.6) Inglewood, LA Basin event. A rupture velocity of 3.5 km/s and a fault length (*fl*) of 1.3 km was determined with rupture to the south, Fig. 1. The rise time was estimated to be .24s. These estimates were obtained from following the CAP+ procedure from the TriNet array at stations outside the Basin. These results are validated by predicting the P-waveforms in the LA Basin with example given in Fig. 1. Station STS is situated to the south, AZ = 142°, while station SMS is to the north, AZ = 307°. The Green star indicates the predictions, see *Luo et al.* (2010) just published for details. We plan to extend these studies to other Basin events and address shallow structure but have become sidetracked by the El Mayor-Cucapah sequence, *Wei et al.* (2011).

References

Luo, Yan, Y. Tan, S. Wei, D. Helmberger, Z. Zhan, S. Ni, E. Hauksson, and Y. Chen (2010). Source Mechanism and Rupture Directivity of the M_w 4.6 May 18, 2008 Inglewood, California Earthquake, *BSSA*, Short Note, **100**, 3269-3277.

Tan, Ying, L. Zhu, D. V. Helmberger, and C. Saikia (2006). Locating and Modeling Regional Earthquakes with Two Stations, *J. Geophys. Res.* **111**(B1):1306-1320.

Tan, Ying and D. V. Helmberger (2007). A New Method for Determining Small Earthquake Source Parameters Using Short-period *P* waves, *Bull. Seismol. Soc. Am.*, **97**, No. 4, 1176-1195.

Tan, Ying and Don Helmberger (2010). Rupture Characteristics of Small Earthquakes; 2003 Big Bear Sequence, *Bull. Seismol. Soc. Am.*, **100**, 2890-2904.

Wei, Shengji, Eric Fielding, Sebastien Leprince, Anthony Sladen, Jean-Philippe Avouac, Don Helmberger, Egill Hauksson, Risheng Chu, Mark Simons, Kenneth Hudnut, Thomas Herring, and Richard Briggs (2011). Superficial simplicity of the 2010 Mw 7.2 El Mayor-Cucapah earthquake of Baja California, Mexico. *Nature*, in press.

Wei, Shengji, Z. Zhan, D. V. Helmberger, Y. Tan, and S. Ni (2011). Rapid Regional Centroid Solutions, *Bull. Seismol. Soc. Am.* submitted.

Zhan, Zhongwen, S. Wei, S. Ni, and Don Helmberger (2011). Earthquake Centroid Locations Using Calibration from Ambient Seismic Noise, *BSSA*, in press.

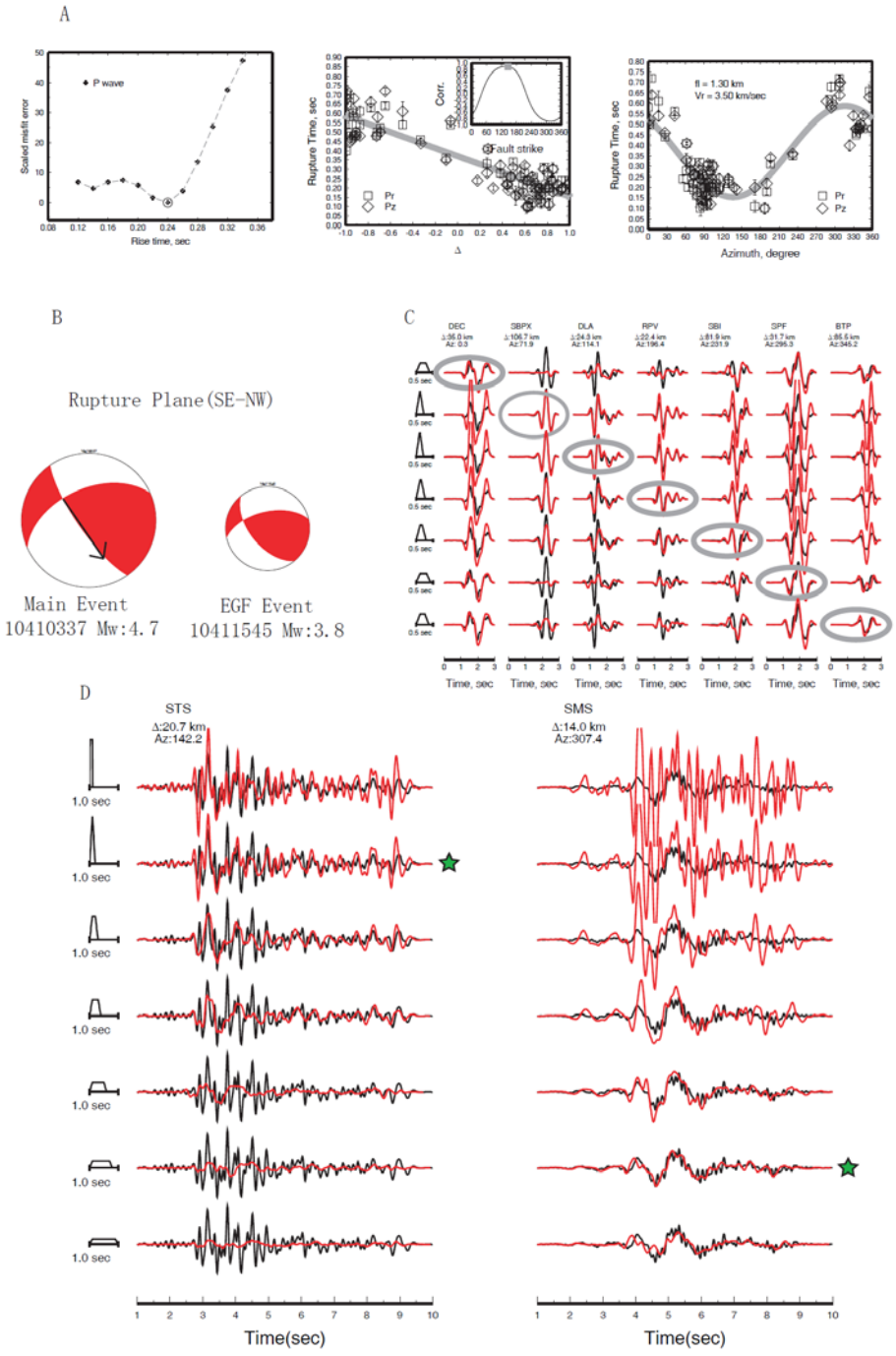

Figure 1. The upper panel displays the directivity inversion on the P-waves and the lower panel shows the prediction at stations SMS (away) and STS (towards). The circle indicates the preferred fit at each station both in waveform shape and amplitude, *Tan and Helmberger* (2010). Because of the high rupture velocity (3.5 km/s), the SH directivity effects at the ends of the fault are obvious. In this case, we used the first 5s of the displacement records assuming the same empirical Green's function (M_w = 3.8) used in the upper panel.